11. Uezono, Y. *et al.* Activation of inwardly rectifying K^+ channels by $GABA_B$ receptors expressed in *Xenopus* oocytes. *Neuroreport* **9,** 583–587 (1998).
12. Couve, A. *et al.* Intracellular retention of recombinant $GABA_B$ receptors. *J. Biol. Chem.* **273,** 26361–26367 (1998).
13. Hill, D. R., Bowery, N. G. & Hudson, A. L. Inhibition of $GABA_B$ receptor binding by guanyl nucleotides. *J. Neurochem.* **42,** 652–657 (1984).
14. Morris, S. J., Beatty, D. M. & Chronwall, B. M. $GABA_B$R1a/R1b-type receptor antisense deoxynucleotide treatment of melanotropes blocks chronic $GABA_B$ receptor inhibition of high-voltage-activated Ca^+ channels. *J. Neurochem.* **71,** 1329–1332 (1998).
15. Kenakin, T. Differences between natural and recombinant G-protein coupled receptor systems with varying receptor/G-protein stoichiometry. *Trends Pharmacol. Sci.* **18,** 456–464 (1997).
16. McLatchie, L. M. *et al.* RAMPs regulate the transport and ligand specificity of the calcitonin-receptor-like receptor. *Nature* **393,** 333–339 (1998).
17. Dwyer, N. D., Troemel, E. R., Sengupta, P. & Bargmann, C. I. Odorant receptor localization to olfactory cilia is mediated by ODR-4, a novel membrane-associated protein. *Cell* **93,** 455–466 (1998).
18. Bischoff, S., Barhanin, J., Bettler, B., Mulle, C. & Heinemann, S. Spatial distribution of kainate receptor subunit mRNA in the mouse basal ganglia and ventral mesencephalon. *J. Comp. Neurol.* **379,** 541–562 (1997).
19. Malitschek, B. *et al.* Developmental changes in agonist affinity at $GABA_B$R1 receptor variants in rat brain. *Mol. Cell. Neurosci.* **12,** 56–64 (1998).
20. Olpe, H.-R. *et al.* CGP 35348: a centrally active blocker of $GABA_B$ receptors. *Eur. J. Pharmacol.* **187,** 27–38 (1990).
21. Shigemoto, R. *et al.* Target-cell-specific concentration of a metabotropic glutamate receptor in the presynaptic active zone. *Nature* **381,** 523–525 (1996).
22. Wischmeyer, E. *et al.* Subunit interactions in the assembly of neuronal Kir3.0 inwardly rectifying K^+ channels. *Mol. Cell. Neurosci.* **9,** 194–206 (1997).
23. Mosbacher, J. *et al.* P2Y receptor subtypes differentially couple to inwardly rectifying potassium channels. *FEBS Lett.* **436,** 104–110 (1998).
24. von Heijne, G. A new method for predicting signal sequence cleavage sites. *Nucleic Acids Res.* **14,** 4683–4690 (1986).
25. O'Hara, P. J. *et al.* The ligand-binding domain in metabotropic glutamate receptors is related to bacterial periplasmic binding proteins. *Neuron* **11,** 41–52 (1993).

Supplementary information is available on *Nature*'s World-Wide Web site (http://www.nature.com) or as paper copy from the London editorial office of *Nature*.

Acknowledgements. We thank D. Ristig, A. Begrich, I. Meigel and S. Leonhard for technical assistance.

Correspondence and requests for materials should be addressed to B.B. (e-mail: bernhard.bettler@pharma.novartis.com). The rat $GABA_B$R2 cDNA sequence has been deposited at EMBL under the accession number AJ011318.

Moderate loss of function of cyclic-AMP-modulated KCNQ2/KCNQ3 K^+ channels causes epilepsy

Björn C. Schroeder*, Christian Kubisch*, Valentin Stein & Thomas J. Jentsch

Zentrum für Molekulare Neurobiologie Hamburg (ZMNH), Universität Hamburg, Martinistrasse 85, D-20246 Hamburg, Germany
* *These authors contributed equally to this work*

Epilepsy affects more than 0.5% of the world's population and has a large genetic component[1]. It is due to an electrical hyperexcitability in the central nervous system. Potassium channels are important regulators of electrical signalling, and benign familial neonatal convulsions (BFNC), an autosomal dominant epilepsy of infancy, is caused by mutations in the *KCNQ2* or the *KCNQ3* potassium channel genes[2–4]. Here we show that KCNQ2 and KCNQ3 are distributed broadly in brain with expression patterns that largely overlap. Expression in *Xenopus* oocytes indicates the formation of heteromeric KCNQ2/KCNQ3 potassium channels with currents that are at least tenfold larger than those of the respective homomeric channels. KCNQ2/KCNQ3 currents can be increased by intracellular cyclic AMP, an effect that depends on an intact phosphorylation site in the KCNQ2 amino terminus. KCNQ2 and KCNQ3 mutations identified in BFNC pedigrees compromised the function of the respective subunits, but exerted no dominant-negative effect on KCNQ2/KCNQ3 heteromeric channels. We predict that a 25% loss of heteromeric KCNQ2/KCNQ3-channel function is sufficient to cause the electrical hyperexcitability in BFNC. Drugs raising intracellular cAMP may prove beneficial in this form of epilepsy.

We cloned the complete complementary DNA of the human KCNQ3 K^+ channel by homology to KCNQ1 (also known as KVLQT1 (ref. 5)) and determined its genomic structure. We identified two intronic CA nucleotide repeats which represent microsatellite markers linked previously to the long arm (q) of chromosome 8 at band 24, one of the known loci[6,7] for BFNC. Indeed, a partial KCNQ3 cDNA was cloned recently and a KCNQ3 mutation was identified in a BFNC family[3]. The KCNQ3 protein (Fig. 1) is 41% identical to KCNQ2, the other K^+ channel mutated in BFNC, and 31% identical to KCNQ1, a K^+ channel subunit mutated in the long QT syndrome[5] (LQTS). It displays the typical structure of a K^+ channel with six transmembrane domains and a pore-forming P-loop.

KCNQ3 shows similarities to KCNQ2 (ref. 2) in being highly specific for brain (Fig. 2a). Northern blot analysis and *in situ* hybridization revealed that both genes are co-expressed in most brain regions, but there are some regional quantitative differences (Fig. 2b). Potassium channels are tetramers of identical or homologous α-subunits[8–10], raising the possibility that KCNQ2 and KCNQ3 form heteromeric channels. After co-expressing KCNQ2 and KCNQ3 that had been N-terminally tagged with haemagglutinin (HA) or Flag epitopes in *Xenopus* oocytes, we were able to co-

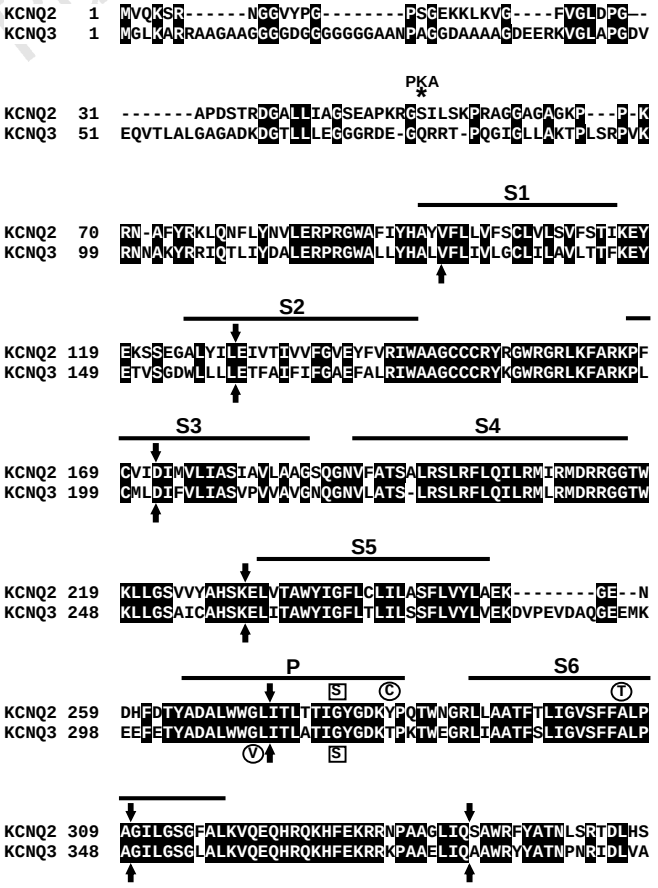

Figure 1 Partial alignment of KCNQ2 and KCNQ3 potassium channel subunits showing the newly identified KCNQ3 N terminus, the cAMP-dependent phosphorylation site (*) in KCNQ2, and the point mutations introduced here. Identical residues are marked by black background. Predicted transmembrane spans S1–S6 and the P-loop (P) are indicated. Positions of introns in both genes are shown by arrows, but the KCNQ2 exon-intron structure is incomplete[2]. The Y284C and A306T (KCNQ2) and G310V (KCNQ3) mutations (circles) were found[3,4] in BFNC pedigrees, whereas the G279S (KCNQ2) and G318S (KCNQ3) mutations (squares) were modelled on mutations in KCNQ1 found[14] in dominant LQTS patients.

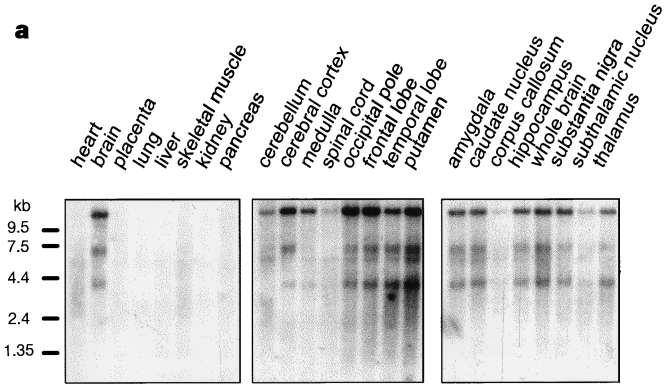

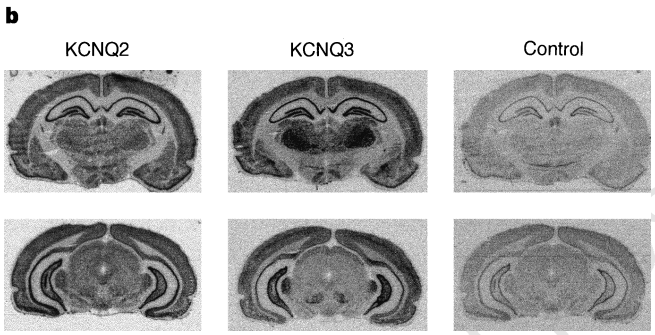

Figure 2 Expression patterns of KCNQ2 and KCNQ3. **a**, Northern blot analysis of KCNQ3 expression. Among the human tissues analysed, KCNQ3 mRNA was found only in brain (left panel). Within brain (centre and right panels), expression occurs in most regions, but transcript levels are low in the spinal cord and corpus callosum. **b**, *In situ* hybridization of rat brain slices with antisense probes directed against KCNQ2 (left) and KCNQ3 (centre). Right panel shows control hybridization with a KCNQ2 sense probe. KCNQ2 and KCNQ3 expression overlaps in large areas of the brain, but KCNQ3 expression is higher in several nuclei, for example the amygdala and thalamic nuclei.

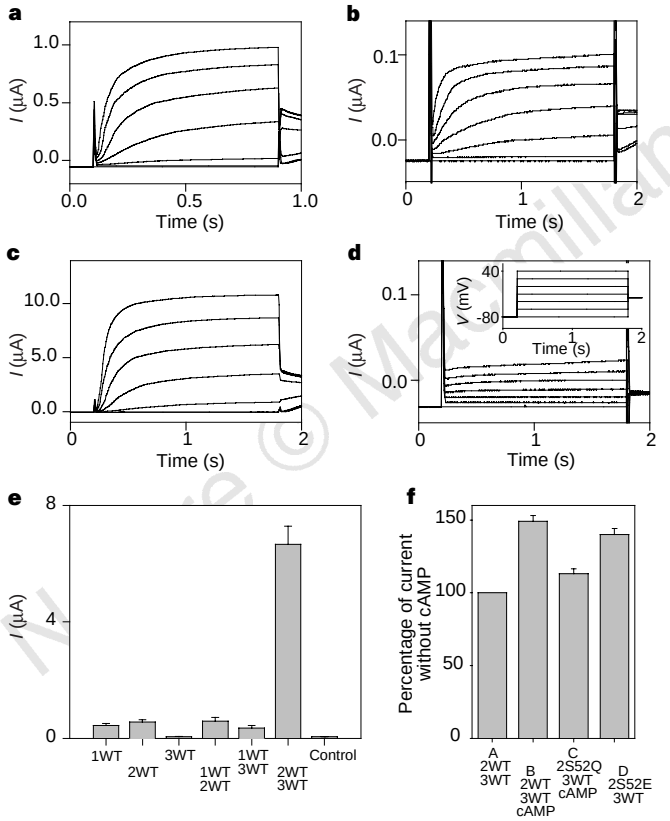

Figure 3 Functional expression of KCNQ channels in *Xenopus* oocytes. **a**, Voltage-clamp traces of KCNQ2. **b**, Traces of KCNQ3. **c**, 1:1 co-expression of KCNQ2 and KCNQ3 (note different scales). **d**, Control oocyte (clamp protocol shown in inset). **e**, Mean currents at +40 mV of different KCNQs (for example, 2WT means KCNQ2 wild type). Measurements are from a single batch of oocytes ($n > 8$, error bars indicate s.e.m.). **f**, Effect of raising intracellular cAMP (see Methods) on currents measured as in **e** (error bars indicate s.e.m.). Currents were normalized to those of the respective oocyte before applying cAMP (bars B, C), or to oocytes of the same batch injected with WT KCNQ2/KCNQ3 (bar D). 2S52Q and 2S52E indicate KCNQ2 mutants deleted for the PKA site or mimicking a phosphorylated PKA site, respectively.

precipitate KCNQ2 with KCNQ3 and vice versa (data not shown).

When expressed in *Xenopus* oocytes, KCNQ3 elicited currents (Fig. 3b) that were only barely above background (Fig. 3d), but resembled the larger depolarization-activated K^+ currents observed[2] with KCNQ2 (Fig. 3a). Co-injection of both cRNAs yielded currents (Fig. 3c) that were at least one order of magnitude larger than those observed with either subunit alone (Fig. 3e). Their voltage dependence and kinetics roughly resembled those of KCNQ1, KCNQ2 and KCNQ3, but seemed less inwardly rectifying than KCNQ2 currents. Currents observed after KCNQ1/KCNQ2 co-expression, however, did not differ significantly from a linear superposition of currents from the respective homomeric channels. KCNQ1 currents are changed markedly by co-expressing minK (IsK)[11,12], but we observed no pronounced effect when we expressed KCNQ2 and KCNQ3 together with this β-subunit at a concentration (0.2 ng per oocyte) sufficient to change KCNQ1 currents (data not shown). The relevance of such an effect would, however, be questionable because minK is not expressed in significant amounts in brain[13].

Because the cytoplasmic N terminus of KCNQ2 contains a consensus site for cAMP-dependent phosphorylation (Fig. 1), we raised the intracellular cAMP concentration by applying cpt-cAMP (8-(4-chlorophenylthio)-cAMP), forskolin and IBMX (3-isobutyl-1-methylxanthine). This reversibly increased currents with wild-type (WT) KCNQ2/KCNQ3 by 49 ± 16% (±s.d.) ($n = 17$) (Fig. 3f, bar B). This increase was largely inhibited by H-89, a blocker of protein kinase A (PKA) (data not shown). A mutation (S52Q) eliminating the potential N-terminal phosphorylation site of KCNQ2 reduced the stimulation by cAMP to 13 ± 12% (±s.d.) ($n = 12$) (Fig. 3f, bar C), indicating that the current increase depends on the phosphorylation of this site. Whereas some oocytes injected with the mutant channel lacked a response to cAMP, in others a small response remained. This indicates that other processes (for example, phosphorylation of alternative sites or endo-exocytosis of channels) may participate in the current stimulation. When we introduced a mutation (S52E) in which the negatively charged glutamate mimics a phosphorylated serine residue, currents were larger by ~40% (25–65%, 128 oocytes from four different batches) (Fig. 3f, bar D). These experiments indicate that the activation of KCNQ2/KCNQ3 channels by cAMP is mediated by PKA. To show this more directly, we exposed excised patches from HEK293 cells expressing both channel subunits to the catalytic subunit of PKA in the presence of Mg-ATP. This led to a large, reversible enhancement of K^+ currents (Fig. 4).

We next investigated the effects of point mutations on the function of homo- and heteromeric channels to understand further

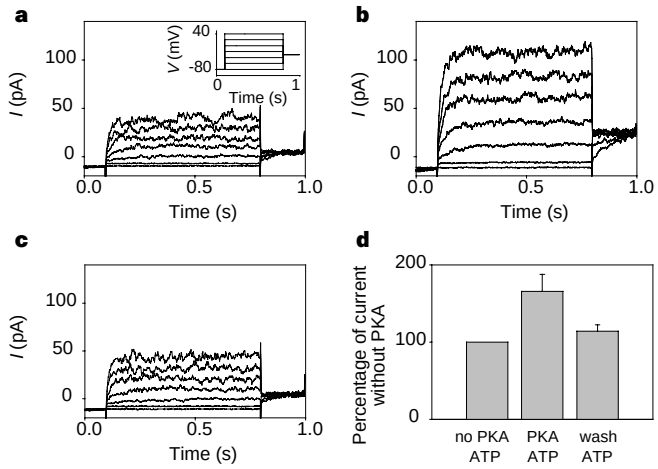

Figure 4 Effect of PKA on KCNQ2/KCNQ3 channels expressed in HEK293 cells. **a–c**, Currents from an inside-out patch in presence of 2 mM Mg-ATP before addition of PKA (**a**), 1 min after addition of PKA (**b**), and after wash-out (**c**). Clamp protocol is shown in the inset in **a**. **d**, Effect of PKA on currents measured as in **a–c** ($n = 6$, error bars indicate s.e.m.). PKA stimulated currents by 66 ± 22% (centre bar). This effect was largely reversible as currents returned to 14 ± 8% above the original level after wash-out (right bar). Currents were normalized to the respective current before applying PKA (left bar).

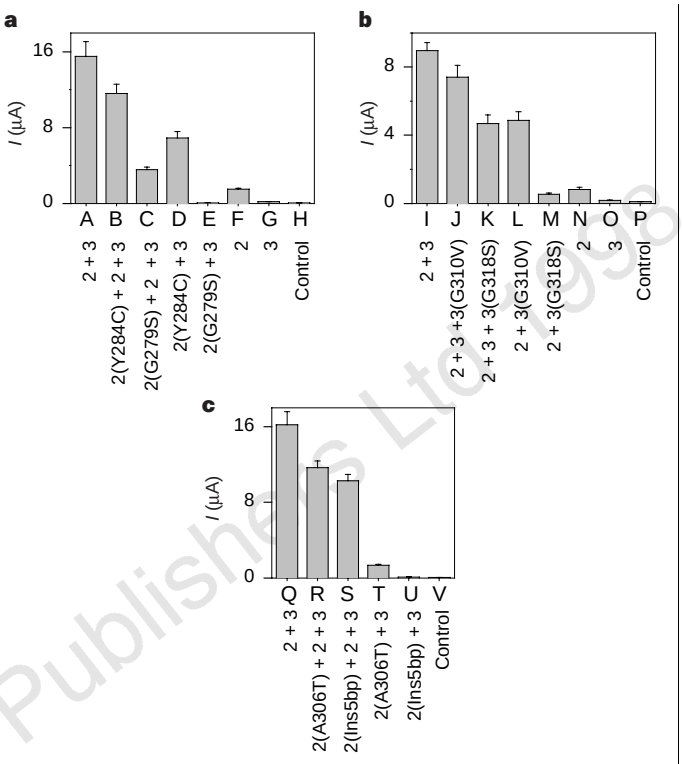

Figure 5 Functional analysis of KCNQ2 and KCNQ3 mutations. Effect of pore mutations in KCNQ2 (**a**) or KCNQ3 (**b**) and of non-pore mutations in KCNQ2 (**c**) on KCNQ2/KCNQ3 currents (same total amount of RNA). KCNQ2(Y284C), KCNQ2(A306T), KCNQ2(ins5bp) and KCNQ3(G310V) are BFNC mutations[2–4], whereas KCNQ2(G279S) and KCNQ3(G318S) mimic a dominant-negative KCNQ1 mutation[14,15]. **a**, KCNQ2(G279S) exerts a strong dominant-negative effect with (bar C) or without (bar E) wild-type KCNQ2. The BFNC mutation KCNQ2(Y284C) lacks a dominant-negative effect (bars B, D), as does KCNQ3(G310V) (**b**, bars J, L). The artificial KCNQ3(G318S) mutation has a dominant-negative effect (bars K, M) (smaller than the one of KCNQ2(G279S) in **a**). In **c**, a mutation in S6 (A306T)[4] and a truncation (1592ins5bp)[2] reduce currents by <40% (bars R and S, respectively). The KCNQ2(ins5bp) mutant did not enhance KCNQ3 currents (bar U). Different batches of oocytes were used in **a**, **b** and **c**. Within each panel, a single batch was used. Bars, mean values from >11 oocytes; error bars, s.e.m.

the pathomechanism of epilepsy. Y284C, a BFNC mutation[4] in the pore region of KCNQ2, did not abolish channel function. Currents were reduced to ~30–60% (not shown), and a 1:1 co-expression with KCNQ3 again yielded much larger currents (Fig. 5a, bar D). To mimic the situation in a (heterozygous) patient with this dominant disease, we injected KCNQ2(Y284C), KCNQ2, and KCNQ3 at a ratio of 1:1:2 (Fig. 5a, bar B). Compared with wild-type KCNQ2/KCNQ3 heteromers, this combination reduced currents by only 20–30%. The only known BFNC mutation in KCNQ3, G310V, also affects a residue in the pore region[3]. We could not detect currents with KCNQ3(G310V), but in view of the low currents of wild-type KCNQ3 this does not prove a total loss of function. When co-injected 1:1 with KCNQ2, we observed large currents that were ~50% of wild-type heteromeric currents (Fig. 5b, bar L). A co-injection scheme mimicking the situation in a heterozygous patient (Fig. 5b, bar J) again resulted in currents reduced by only 20% compared with wild type. In addition to these pore mutations, we tested the effect of a KCNQ2 missense mutation (A306T)[4] in transmembrane domain S6 and of an insertion of five base pairs (1592ins5bp)[2] in the carboxy terminus of KCNQ2 that leads to a truncated protein. Both mutations cause BFNC (refs 2, 4). Again, when co-expressed with wild-type KCNQ2 and KCNQ3 at a 1:1:2 ratio, the reduction in currents was in the range of 20–40% (Fig. 5c, bars R, S). On the basis of titration experiments (not shown), similar reductions in currents would be expected in patients with a deletion of KCNQ2 on one allele[4]. In all cases, we did not observe physiologically significant changes in ion selectivity or gating kinetics with mutant/wild-type heteromeric channels. This includes heteromeric channels with mutations in the P-loop, which retained the high K^+/Na^+ permeability ratio (>40) of wild-type channels. Thus, none of these BFNC mutations exerted a dominant-negative effect (defined by a current reduction of >50%).

To contrast the behaviour of BFNC mutants with a dominant-negative effect, we constructed KCNQ2(G279S) and KCNQ3(G318S). These mutations were modelled on KCNQ1(G291S), a pore mutation that is found[14] in the dominant Romano–Ward LQTS and which has a dominant-negative effect[15]. In contrast to the BFNC mutants studied above, these mutants exerted a dominant-negative effect on heteromeric channels both in the presence and in the absence of the respective wild-type subunit (Fig. 5a, b). The inhibitory effect of the KCNQ2 mutant was somewhat larger.

The overlapping expression pattern, the ability to associate physically, the large increase in currents upon co-expression, and the observation that mutations in *KCNQ2* and *KCNQ3* cause clinically identical diseases suggest that BFNC is due to a loss of KCNQ2/KCNQ3 heteromeric channels. Surprisingly, our experiments predict that this loss of function is quite small. This applies for missense mutations as well as for C-terminal deletions and gene deletions, both of which are rather common mutation types[2,4] in BFNC. This is in contrast to the dominant LQTS, where mutations in *KCNQ1* act in a dominant-negative manner[13,15]. It is tempting to speculate that dominant-negative mutations in *KCNQ2* or *KCNQ3* may lead to more severe phenotypes. The slight loss of channel function predicted for BFNC patients implies that expression levels of KCNQ2/KCNQ3 channels are at a critical level during the early period of life in which this transient form of epilepsy occurs. The fact that the stimulation of KCNQ2/KCNQ3 currents by cAMP is within the range of the reduction of currents in BFNC suggests new ways in which this and possibly other forms of epilepsies may be treated pharmacologically. □

Methods

Cloning of KCNQ3 and generation of mutants. Expressed sequence tags (IMAGE Consortium cDNA clones[16], accession numbers AA001392, AA019129 and H86050) homologous to KCNQ1 were extended at both ends by screening human brain cDNA libraries and by polymerase chain reaction (PCR) after reverse transcription of RNA (RT-PCR) techniques. The start ATG was assigned to the first ATG in frame following an upstream stop codon. The cDNA was inserted into the expression vector PTLN (ref. 17) which uses *Xenopus* β-globin untranslated sequences to boost expression in *Xenopus* oocytes. The genomic structure of KCNQ3 was determined by amplifying genomic sequences from human DNA using exonic primers and sequencing the products. The sequence of KCNQ3 exons and adjacent intronic stretches were deposited in the GenBank/EMBL database (accession numbers AF071478–AF071491). In introns 1 and 7, we discovered the microsatellite markers D8S558 and D8S1835 that map to chromosome 8q24. Mutagenesis was done using recombinant PCR and the *Pfu* DNA polymerase. Constructs were verified by sequencing using ABI 377 or 310 automated sequencers.

Analysis of tissue distribution. For northern blot analysis, we used human RNA blots (Clontech) and a radiolabelled 526-base-pair *Not*I/*Hin*dIII fragment from KCNQ3 as a probe. For *in situ* hybridization, 1.5-kilobase antisense and control sense RNA probes labelled with ^{35}S were transcribed by T3 or T7 RNA polymerases from KCNQ2 and KCNQ3 partial clones in pBluescript using the Maxiscript kit (Ambion). Template DNA and unincorporated nucleotides were removed. Probe sizes were reduced by controlled alkaline treatment. *In situ* hybridization was done as described[18], with the following modifications: after washing in PBS, sections were acetylated without ultraviolet crosslinking, and were exposed to Kodak Biomax X-ray film.

Expression in *Xenopus* oocytes and HEK cells and electrophysiology. After linearization of the constructs, capped cRNA was synthesized using SP6 RNA polymerase and the mMessage mMachine kit (Ambion). For KCNQ1, we used isoform 0 (ref. 15). *Xenopus* oocytes were prepared, injected (generally with 5 ng cRNA), and handled as described[19]. After 1–2 days, currents were examined at room temperature in saline containing (in mM) 96 NaCl, 2 KCl, 3 $MgCl_2$, 0.2 $CaCl_2$, and 5 HEPES (pH 7.4) using two-electrode voltage clamping with a TurboTec amplifier (NPI). To raise intracellular cAMP, we applied 200 μM cpt-cAMP, 10 μM forskolin and 1 mM IBMX for 15 min. For kinase inhibition, oocytes were exposed for >6 h to 100 μM H-89 (Calbiochem). HEK 293 cells were transiently transfected with KCNQ2 and KCNQ3 cDNAs subcloned into pCDNA3 (Invitrogen) using Lipofectamin (Gibco). The inside-out configuration of the pach-clamp technique was used with borosilicate glass pipettes (5 MΩ resistance) and an Axopatch 200-A amplifier (Axon). Currents were filtered at 250 Hz, digitally sampled at 500 Hz, and analysed with pClamp (Axon) and Sigma Plot (Jandel Scientific) software. The bath solution contained, in mM: 140 K, 140 aspartic acid, 2 $MgCl_2$, 5 HEPES, 2 EGTA (pH 7.3 adjusted with KOH); pipette solution: 140 Na, 5 K, 145 aspartic acid, 2 $CaCl_2$, 2 $MgCl_2$, 5 HEPES (pH 7.3 adjusted with NaOH). Excised patches were superfused with bath solution containing 2 mM Mg-ATP or 2 mM Mg-ATP and 40 U m^{-1} PKA catalytic subunit from bovine heart (Calbiochem) where noted.

Received 21 September; accepted 3 November 1998.

1. Baraitser, M. in *The Genetics of Neurological Disorders* 2nd edn (*Oxf. Monogr. Med. Genet.*, No. 18) 96–113 (Oxford Univ. Press, New York, 1990).
2. Biervert, C. *et al.* A potassium channel mutation in neonatal human epilepsy. *Science* **279,** 403–406 (1998).
3. Charlier, C. *et al.* A pore mutation in a novel KQT-like potassium channel in an idiopathic epilepsy family. *Nature Genet.* **18,** 53–55 (1998).
4. Singh, N. A. *et al.* A novel potassium channel gene, *KCNQ2*, is mutated in an inherited epilepsy of newborns. *Nature Genet.* **18,** 25–29 (1998).
5. Wang, Q. *et al.* Positional cloning of a novel potassium channel gene: *KVLQT1* mutations cause cardiac arrhythmias. *Nature Genet.* **12,** 17–23 (1996).
6. Leppert, M. *et al.* Benign familial neonatal convulsions linked to genetic markers on chromosome 20. *Nature* **337,** 647–648 (1989).
7. Lewis, T. B., Leach, R. J., Ward, K., O'Connell, P. & Ryan, S. G. Genetic heterogeneity in benign familial neonatal convulsions: identification of a new locus on chromosome 8q. *Am. J. Hum. Genet.* **53,** 670–675 (1993).
8. Christie, M. J., North, R. A., Osborne, P. B., Douglass, J. & Adelman, J. P. Heteropolymeric potassium channels expressed in *Xenopus* oocytes from cloned subunits. *Neuron* **2,** 405–411 (1990).
9. Isacoff, E. Y., Jan, Y. N. & Jan, L. Y. Evidence for the formation of heteromultimeric potassium channels in *Xenopus* oocytes. *Nature* **345,** 530–534 (1990).
10. Ruppersberg, J. P. *et al.* Heteromultimeric channels formed by rat brain potassium-channel proteins. *Nature* **345,** 535–537 (1990).
11. Barhanin, J. *et al.* K_VLQT1 and IsK (minK) proteins associate to form the I_{Ks} cardiac potassium current. *Nature* **384,** 78–80 (1996).
12. Sanguinetti, M. C. *et al.* Coassembly of K_VLQT1 and minK (IsK) proteins to form cardiac I_{Ks} potassium channel. *Nature* **384,** 80–83 (1996).
13. Chouabe, C. *et al.* Properties of K_VLQT1 K^+ channel mutations in Romano-Ward and Jervell and Lange-Nielsen inherited cardiac arrhythmias. *EMBO J.* **16,** 5472–5479 (1997).
14. Russell, M. W., Macdonald, D., Collins, F. S. & Brody, L. C. KVLQT1 mutations in three families with familial or sporadic long QT syndrome. *Hum. Mol. Genet.* **5,** 1319–1324 (1996).
15. Wollnik, B. *et al.* Pathophysiological mechanisms of dominant and recessive *KVLQT1* K^+ channel mutations found in inherited cardiac arrhythmias. *Hum. Mol. Genet.* **6,** 1943–1949 (1997).
16. Lennon, G., Auffray, C., Polymeropoulos, M. & Soares, M. B. The I.M.A.G.E. Consortium: an integrated molecular analysis of genomes and their expression. *Genomics* **33,** 151–152 (1996).
17. Lorenz, C., Pusch, M. & Jentsch, T. J. Heteromultimeric CLC chloride channels with novel properties. *Proc. Natl Acad. Sci. USA* **93,** 13362–13366 (1996).
18. Hartmann, D., Fehr, S., Meyerhof, W. & Richter, D. Distribution of somatostatin receptor subtype 1 mRNA in the developing cerebral hemispheres of the rat. *Dev. Neurosci.* **17,** 246–255 (1995).
19. Jordt, S.-E. & Jentsch, T. J. Molecular dissection of gating in the ClC-2 chloride channel. *EMBO J.* **16,** 1582–1592 (1997).

Acknowledgements. We thank S. Fehr for the preparation of rat brain slices and the *in situ* hybridization, and T. Friedrich for comments on the manuscript. This work was supported by grants from the Deutsche Forschungsgemeinschaft and the Fonds der Chemischen Industrie to T.J.J.

Correspondence and requests for materials should be addressed to T.J.J. (e-mail: jentsch@plexus.uke.uni-hamburg.de).

Changes in thymic function with age and during the treatment of HIV infection

Daniel C. Douek*, Richard D. McFarland†, Philip H. Keiser*, Earl A. Gage*, Janice M. Massey‡, Barton F. Haynes‡, Michael A. Polis§, Ashley T. Haase‖, Mark B. Feinberg¶, John L. Sullivan#, Beth D. Jamieson☆, Jerome A. Zack☆, Louis J. Picker† & Richard A. Koup***

*Departments of * Medicine and † Pathology, The University of Texas Southwestern Medical Center, Dallas, Texas 75235, USA*
‡ Department of Medicine, Duke University Medical Center, Durham, North Carolina 27710, USA
§ National Institute of Allergy and Infectious Diseases, National Institutes of Health, Bethesda, Maryland 20892, USA
‖ Department of Microbiology, University of Minnesota Medical School, Minneapolis, Minnesota 55455, USA
¶ Department of Medicine, Emory University School of Medicine, Atlanta, Georgia 3022, USA
 # Departments of Pediatrics and Molecular Medicine, The University of Massachusetts Medical Center, Worcester, Massachusetts 01605, USA
☆ Division of Hematology-Oncology, Department of Medicine, and
*** Department of Microbiology and Molecular Genetics, UCLA School of Medicine and UCLA Institute, Los Angeles, California 90095, USA*

The thymus represents the major site of the production and generation of T cells expressing αβ-type T-cell antigen receptors[1]. Age-related involution[2] may affect the ability of the thymus to reconstitute T cells expressing CD4 cell-surface antigens that are lost during HIV infection[3]; this effect has been seen after chemotherapy and bone-marrow transplantation[4,5]. Adult HIV-infected patients treated with highly active antiretroviral therapy (HAART) show a progressive increase in their number of naive CD4-positive T cells[6,7]. These cells could arise through expansion of existing naive T cells in the periphery[8] or through thymic production of new naive T cells[9,10]. Here we quantify thymic output by measuring the excisional DNA products of TCR-gene rearrangement. We find that, although thymic function declines with age, substantial output is maintained into late adulthood. HIV infection leads to a decrease in thymic function that can be measured in the peripheral blood and lymphoid tissues. In adults treated with HAART, there is a rapid and sustained increase in thymic output in most subjects. These results indicate that the adult thymus can contribute to immune reconstitution following HAART.

In humans, there is no known way to distinguish phenotypically between cells that have recently emigrated the thymus and long-